

Article

Not peer-reviewed version

Theoretical Study of The Halogen Concentration Effect on The 1,3-Butadiene Polymerization Catalyzed by the Neodymium-Based Ziegler–Natta System

[Alexey N. Masliy](#)*, Ildar G. Akhmetov, Andrey M. Kuznetsov, [Ilsiya M. Davletbaeva](#)

Posted Date: 11 September 2024

doi: 10.20944/preprints202409.0893.v1

Keywords: DFT; ONIOM; 1,3-butadiene polymerization; stereospecificity; cis-1,4-polybutadiene; neodymium based Ziegler–Natta catalyst



Preprints.org is a free multidiscipline platform providing preprint service that is dedicated to making early versions of research outputs permanently available and citable. Preprints posted at Preprints.org appear in Web of Science, Crossref, Google Scholar, Scilit, Europe PMC.

Copyright: This is an open access article distributed under the Creative Commons Attribution License which permits unrestricted use, distribution, and reproduction in any medium, provided the original work is properly cited.

Disclaimer/Publisher's Note: The statements, opinions, and data contained in all publications are solely those of the individual author(s) and contributor(s) and not of MDPI and/or the editor(s). MDPI and/or the editor(s) disclaim responsibility for any injury to people or property resulting from any ideas, methods, instructions, or products referred to in the content.

Article

Theoretical Study of the Halogen Concentration Effect on the 1,3-Butadiene Polymerization Catalyzed by the Neodymium-Based Ziegler–Natta System

Alexey N. Masliy ^{1,*}, Ildar G. Akhmetov ², Andrey M. Kuznetsov ¹ and Ilsiya M. Davletbaeva ³

¹ Department of Inorganic Chemistry, Kazan National Research Technological University, 420015, Kazan, K. Marx Street 68, Russia

² Nizhnekamsk Chemical and Technological Institute (branch), Kazan National Research Technological University, 420015, Kazan, K. Marx Street 68, Russia

³ Technology of Synthetic Rubber Department, Kazan National Research Technological University, 420015, Kazan, K. Marx Street 68, Russia

* Correspondence: masliy@kstu.ru (A.N.M.)

Abstract: In this work, an attempt is made to theoretically substantiate the experimentally known facts of the influence of halogen concentration on the catalytic properties of the neodymium-based Ziegler–Natta system. Based on the structural and thermochemical data obtained using modern methods of quantum chemistry, the process of the 1,3-butadiene *cis*-1,4-polymerization under the model active centers of the neodymium Ziegler–Natta catalysts with different content of chloride ions was studied. Results are presented that explain the increase in the *cis*-stereospecificity and activity of the polymerization system with an increase in the content of the chloride ions in the neodymium catalytic system. There were established the reasons for the decrease in the concentration of active centers relative to the introduced Nd(III) with an excess of chloride ions and the occurrence of the *anti-syn* isomerization as a source of the formation of the *trans*-1,4-structures in the *cis*-1,4-polybutadiene.

Keywords: DFT; ONIOM; 1,3-butadiene polymerization; stereospecificity; *cis*-1,4-polybutadiene; neodymium based Ziegler–Natta catalyst

1. Introduction

The creation of Ziegler–Natta catalysts laid the foundation for the industrial production of stereoregular synthetic rubbers [1,2]. Over the past three decades, technologies for the production of SR using lanthanide, primarily neodymium, ion-coordination type catalysts have been actively developed [3–8]. This is due to the unique capabilities of the neodymium catalytic systems, such as their versatility, high activity, stereoregularity and the ability to regulate the molecular weight characteristics of the synthesized polydienes [9–12]. In industrial practice, for the production of synthetic rubbers, as a rule, double [13–17] and triple [18–21] neodymium catalytic systems are used. Depending on the synthesis conditions and the type of initial catalyst components, the properties of the catalytic system and, accordingly, the polymer formed during the polymerization process can be varied over a wide range.

Despite the diversity of the starting components of double and ternary lanthanide catalytic systems, researchers agree on similar models of the structure of active polymerization sites. In our opinion, Yu.B. Monakov's group has advanced most deeply in understanding the structure of the neodymium catalytic systems for the polymerization of dienes [22–24]. They found that the neodymium based Ziegler–Natta catalytic systems are polycentered and can contain up to six types of active centers in their structure. Depending on the synthesis conditions, the catalytic system contains a certain set of active centers. At the same time, one of the key parameters is the halogen content, primarily chlorine, in the Nd(III) coordination sphere. It was found that the maximum *cis*-1,4-stereospecificity of catalytically active centers corresponds to the structure with the highest

chlorine content in the Nd(III) environment and, on the contrary, decreases until inversion to *trans*-stereospecificity with a decrease in the chlorine content in the active center [25,26].

This work is the continuation of the research using modern methods of quantum chemistry, in which, based on structural and thermochemical data, a theoretical justification of the existing experimental data is carried out [27,28] with the aim of further creating new effective industrial neodymium based Ziegler-Natta catalysts.

The data given in Table 1 [29–31] were used as experimental kinetic parameters of the polymerization process of 1,3-butadiene and microstructure of the resulting polybutadiene obtained at various [Cl]:[Nd] molar ratios in the neodymium catalyst.

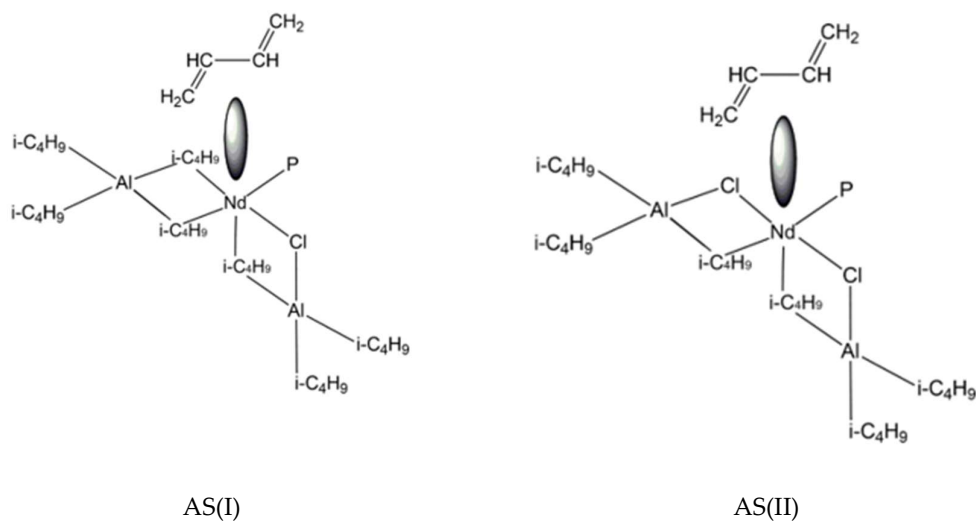
Table 1. – Kinetic parameters of 1,3-butadiene polymerization and microstructure of polybutadiene obtained at different [Cl]:[Nd] molar ratios.

[Cl]:[Nd]	W_p , mol/(l min)	k_g , l/(mol min)	γ_{Nd} , %	<i>cis</i> -1,4- content, %	<i>trans</i> -1,4- content, %	1,2- content, %
1.0	0.03	520	18	95.5	3.4	1.1
2.0	0.18-0.20	2900-2950	32-37	96.0-96.5	2.5-3.0	1.0
3.0	0.25-0.28	4800-4950	27-29	97.1	1.9	1.0
4.0	0.14-0.16	4800-5187	13-17	98.1	0.9	1.0

where: W_p – polymerization rate; k_g – growth rate constant; γ_{Nd} – the proportion of neodymium in active centers.

According to the data given in Table 1, in the studied range of [Cl]:[Nd] ratios, the catalytic system under consideration is *cis*-stereoregulatory. As the inner coordination sphere of Nd(III) becomes saturated with chlorine ions, the growth rate constant of the polymer chain monotonically increases. At the same time, the overall rate of the polymerization process changes extremely, reaching a maximum at the [Cl]:[Nd] ratio of 3, which is due to a change in the proportion of active centers (AS) relative to the introduced Nd(III). The microstructure of the polymer correlates with the chlorine content in the catalyst, an increase in which leads to an increase in the content of *cis*-1,4 structures in the polymer. Experimental data indicate that each [Cl]:[Nd] ratio in the catalyst is characterized by its own set of active centers with a predominant content of centers of a certain type, which has its own kinetic parameters and forms a polymer with certain characteristics.

In accordance with the analysis of literature data and experimental results [25–28], Figure 1 shows models of the active centers of the neodymium catalytic system in which the chlorine content changes. Previously, in [27] a detailed structural and thermochemical analysis of the active center model – AS(IV) was carried out, and the mechanism of its catalytic action was studied. The results of the study not only confirmed the efficiency of the model, but also made it possible to propose a refinement of the classical mechanism of *cis*-stereoregulation of a growing polymer chain.



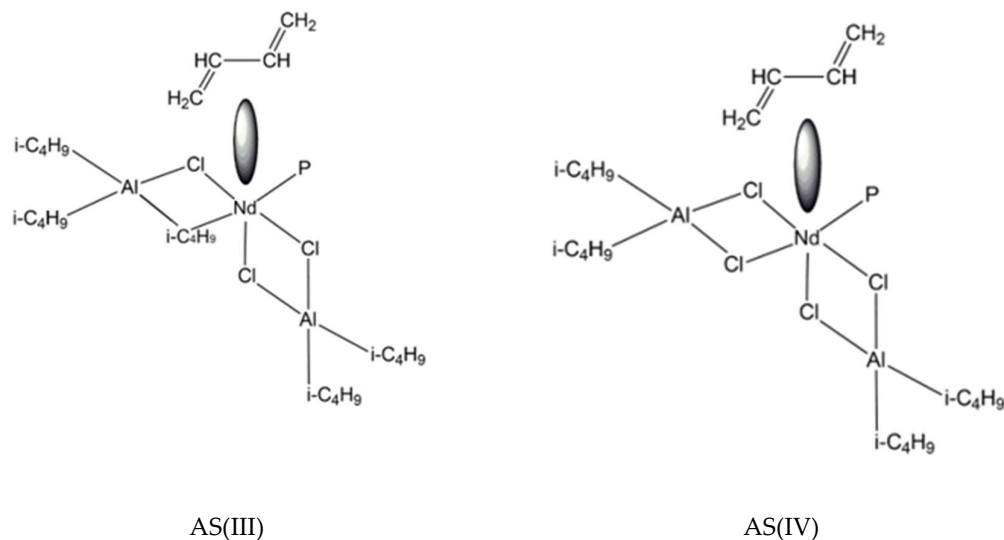


Figure 1. – Models of the neodymium based Ziegler–Natta catalytic systems active centers (AS). P – growing polymer chain / *i*-C₄H₉.

2. Computational Details

Since this work is a direct continuation of our previous studies [27,28], the same methods and approaches were used here.

Quantum-chemical calculations were carried out using the Orca 5.0.3 program package [32,33] in the framework of the ONIOM two layer (QM1/QM2) model [34], in which a part is allocated in the system under study, calculated using the high-level quantum chemical method QM1, and the entire system as a whole is calculated using the low-level QM2 method. Then the results of these two calculations are combined using a special technique. The hybrid density functional B3LYP [35,36] was used as a high-level method (QM1) in the calculations in combination with the second-generation split-valence triple- ζ atomic basis set def2-TZVP by Ahlrichs et al. [37,38]. The core electrons of neodymium atom were described using the def2-ECP pseudopotential [39] recommended for use with def2 basis sets. The tight-binding DFT (semi-empirical DFT) method XTB1 by Grimme et al. [40,41] was chosen as a low-level QM2 method. Since the Nd(III) ion has three unpaired electrons and the total multiplicity of all the complexes under study is 4 (confirmed by a series of additional calculations), the spin-unrestricted method was used for all calculations.

A feature of the systems under study is that weak Van-der-Waals interactions play an important role in them, which were taken into account in the framework of D3 semiempirical model [42] by Grimme et. al.

All calculations were performed with full optimization of molecular geometry without any symmetry constraints. Geometry optimization was carried out taking into account the influence of the solvent (hexane) in the continuum model ALPB – a method of analytical linearization of the Poisson-Boltzmann equation [43].

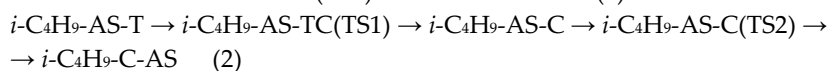
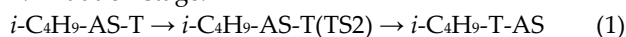
The calculations of vibrational spectra performed after geometry optimization did not contain imaginary modes. This means that the structures found correspond to minima on the total potential energy surface. These calculations were also used to estimate the thermal corrections needed to calculate the total Gibbs free energy of particles (at 298.15 K and 1 atm).

To calculate the activation energies of the process, we used the standard procedure for searching for the transition state. The calculations of vibrational spectra performed after geometry optimization did not contain imaginary modes for minima and contained one imaginary mode for transition states. Each found transition state was checked for compliance with the considered chemical process using the internal reaction coordinate (IRC) procedure.

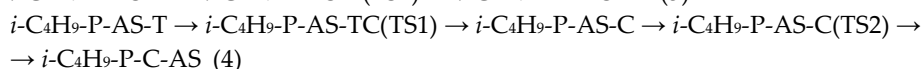
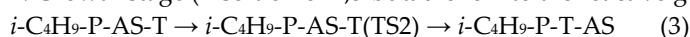
3. Results and Discussion

In this work, the process of *cis*-1,4-polymerization of 1,3-butadiene under the action of model active centers AS(I), AS(II), AS(III) and AS(IV) containing 1, 2, 3 and 4 chlorine atoms in the Nd(III) coordination sphere, respectively was studied. The analysis of the structural characteristics and thermodynamic features of the formation of the AS(IV) complex with 1,3-butadiene, carried out in [34], and the calculation of changes in the activation energy and Gibbs free energy of the polymerization process in this system made it possible to quite reasonably assume the following stages of the formation of 1,4- polybutadiene. The first stage involves the coordination of η -*trans*-C₄H₆ on the active site; then, in the case of the formation of *cis*-1,4-polybutadiene in the region of the coordination interaction, *trans-cis* isomerization of *trans*-1,3-butadiene occurs and, finally, the insertion of 1,3-butadiene into the reactive growing polymer chain takes place. Based on this, the main routes of the stages of initiation and growth of the polymer chain, taking into account the transition states for the systems under study during the formation of 1,4-polybutadiene, can be represented by the following schemes:

1. Initiation stage:



2. Growth stage (insertion of 1,3-butadiene into the reactive growing polymer chain):



where: AS – AS(I), AS(II), AS(III) or AS(IV); T – η -*trans*-C₄H₆ or π -*syn*-C₄H₆; C – η -*cis*-C₄H₆ or π -*anti*-C₄H₆; P – growing polymer chain; TS1 – transition state caused by the *trans-cis* transformation of 1,3-butadiene; TS2 – transition state caused by the insertion of 1,3-butadiene into the reactive growing polymer chain.

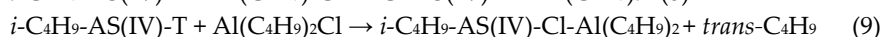
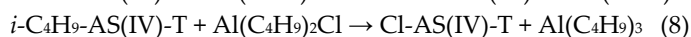
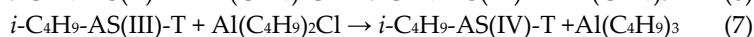
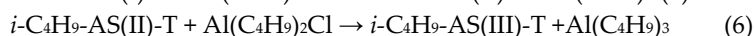
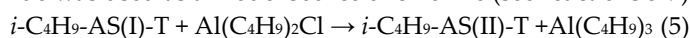
Let's consider the initiation step for AS(I), AS(II), AS(III) and AS(IV), where the calculated Gibbs free energies of reactions 1 and 2 are given in Table 2.

Table 2. Gibbs free energy and activation energy (kJ/mol) of the initiation stage for AS(I)-AS(IV).

Initial structure	ΔG^\ddagger (<i>trans-cis</i>)	ΔG (<i>trans-cis</i>)	ΔG^\ddagger (polymer)	ΔG^\ddagger (total)	ΔG (polymer)	Product
<i>i</i> -C ₄ H ₉ -AS(I)-T	41.4	10.4	64.9	75.3	-38.0	<i>i</i> -C ₄ H ₉ -C-AS(I)
<i>i</i> -C ₄ H ₉ -AS(I)-T			81.6	81.6	-70.3	<i>i</i> -C ₄ H ₉ -T-AS(I)
<i>i</i> -C ₄ H ₉ -AS(II)-T	43.9	12.8	56.8	69.6	-66.6	<i>i</i> -C ₄ H ₉ -C-AS(II)
<i>i</i> -C ₄ H ₉ -AS(II)-T			87.9	87.9	-54.8	<i>i</i> -C ₄ H ₉ -T-AS(II)
<i>i</i> -C ₄ H ₉ -AS(III)-T	41.1	11.4	59.2	70.6	-61.9	<i>i</i> -C ₄ H ₉ -C-AS(III)
<i>i</i> -C ₄ H ₉ -AS(III)-T			86.2	86.2	-51.5	<i>i</i> -C ₄ H ₉ -T-AS(III)
<i>i</i> -C ₄ H ₉ -AS(IV)-T	43.0	6.6	54.3	60.9	-51.7	<i>i</i> -C ₄ H ₉ -C-AS(IV)
<i>i</i> -C ₄ H ₉ -AS(IV)-T			67.0	67.0	-55.1	<i>i</i> -C ₄ H ₉ -T-AS(IV)

As can be seen from the data given in Table 2 for the AS(I), AS(II) and AS(III) complexes, the same trend is observed as for AS(IV), namely that the total activation energy of the initiation stage by introducing 1,3-butadiene in the *cis*-form is lower than when forming the *i*-C₄H₉-T-AS structure. Among other features, it should be noted that the *trans-cis* isomerization of coordinately bound 1,3-butadiene on all active centers proceeds with approximately the same activation energy ~41-44 kJ/mol, while the most favorable structure is characteristic of the active center with the maximum chlorine content.

The highest total activation energy for the process of the insertion of 1,3-butadiene into the reactive growing polymer chain, according to the reaction (2) is observed for AS(I). At the same time, AS(II) and AS(III) have approximately the same total activation energy, which is 5 kJ/mol less in comparison with AS(I). AS(IV) has the lowest total activation energy, which is approximately 10 kJ/mol less than that of AS(II). Also, the highest total activation energy for the process of the insertion of 1,3-butadiene into the reactive growing polymer chain in the form of a *trans*-unit is observed for AS(II). For AS(III) this activation energy is lower by only 1.7 kJ/mol, and for AS(I) it is lower by another 5 kJ/mol. As in the case of reaction (2), for reaction (1) AS(IV) has the lowest activation energy, and this value is 14 kJ/mol lower than that of AS(I). As for the products of reactions (1) and (2), the following trend is observed here: for AS(IV), the *cis*- and *trans*-forms of the final polymer unit at the initiating stage have almost the same stability, with a slight (~ 3 kJ/mol) advantage *trans*-forms. For AS(II) and AS(III), the situation is similar, but the *cis*-form of the terminal unit has greater stability with an advantage of ~10 kJ/mol. At the same time, for AS(I) the situation is fundamentally different; here, the *trans*-form of the terminal unit is approximately twice as advantageous as the *cis*-form. This is consistent with the increase in the proportion of active centers relative to the introduced neodymium at [Cl]:[Nd] in the range from 1.0 to 2.0, but does not correlate with a further decrease in the AS concentration with increasing chlorine content (Table 1). To explain this, the energy characteristics of model AS structures were additionally studied by calculating the thermodynamic parameters of the reactions of a gradual increase in the chlorine content in AS. Diisobutylaluminum chloride was used as a model source of chlorine (see reactions 5-9):



In this case, reactions 5-7 represent a step-by-step transition from AS (I) to AS(IV), and reactions 8 and 9 model the so-called "excess chlorination" of AS (IV) and represent the formation of complexes that are not active in the polymerization process (Figure 2).

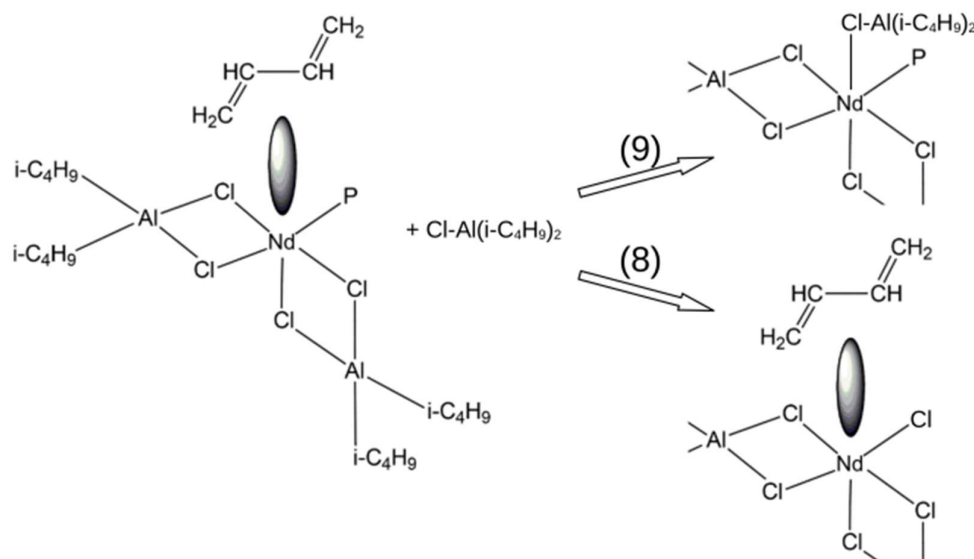


Figure 2. – Models of structures formed by reactions 8 and 9. P – growing polymer chain / *i*-C₄H₉. A fragment of the AS is shown in the right part of the picture for clarity.

The obtained thermodynamic parameters of the reactions 5–9 are given in Table 3. It can be seen that all reactions are exothermic and also have a negative change in Gibbs free energy (with the exception of reaction 9), that is, they must proceed under standard conditions. Thus, structures with

the more chlorine content should be more stable. This is confirmed by an increase in the proportion of active centers during the transition from AS(I) to AS(II). However, a further increase in the chlorine content in the catalytic system and the transition from AS(II) to AS(III) and further to AS(IV) is accompanied by a decrease in the concentration of AS capable of reacting polymerization. Most likely, this is due to the formation of structures in which there is no possibility of the initiation stage occurring, namely the formation of structures in which the chlorinating agent displaces the terminal isobutyl fragment in reaction 8 or replaces 1,3-butadiene in reaction 9. As can be seen from the data obtained, reaction 8 proceeds quite efficiently, and reaction 9 is theoretically possible. It should be noted that the change in entropy in reactions 5–7 has a positive value and suggests that, according to calculations, the process of transforming of active centers from the AS(I) to AS(IV) state is irreversible. In general, the results presented in Table 3 for the first time reasonably explain the decrease in catalyst activity during “excessive chlorination” and can be the subject of a separate study, which will consider not only AS(IV), but also other types of AS.

Table 3. Thermodynamic parameters of the reactions (5–9).

Reaction parameter	Reaction no.				
	5	6	7	8	9
ΔH^{0}_{298} , kJ/mol	-33.5	-41.6	-89.1	-76.8	-8.4
ΔS^{0}_{298} , J/(mol·K)	18.1	13.3	15.6	-11.7	-33.6
ΔG^{0}_{298} , kJ/mol	-38.9	-47.5	-93.7	-73.3	1.5

Summing up the consideration of the stage of the 1,3-butadiene polymerization process initiation under the influence of the model structures of the active centers AS(I), AS(II), AS(III) and AS(IV), we can conclude that the introduction of the first 1,3-butadiene molecule is already characterized by the formation of the π -anti-C₄H₆-AS complex, as a future fragment of the *cis*-1,4-unit of the polymer chain. An increase in the molar ratio [Cl]:[Nd] from 1.0 to 4.0 in the AS structure is accompanied by a decrease in the Gibbs energy of the resulting structures and a decrease in the total activation energy of the initiation stage, that is, an increase in its efficiency. At the same time, the observed decrease in the proportion of active centers relative to the introduced Nd(III) at the [Cl]:[Nd] ratio of 3.0 and 4.0 is explained by the formation of structures that are inactive during the polymerization process.

Next, we considered the stage of polymer chain growth. Since it was previously shown that the stabilization of the calculated values of the energy parameters of the system occurs after the formation of the Kuhn segment, which is a polymer fragment of the three monomer units, it was decided to proceed directly to this stage. AS(IV) structures obtained in [34] were used as a model for the starting compounds. In order not to consider all possible complexes, it was decided to study only the process of adding of 1,3-butadiene to the *i*-C₄H₉-CC-AS and *i*-C₄H₉-CT-AS complexes. Additionally, for all AS, the formation of the *i*-C₄H₉-CCCC-AS structure was considered. The results obtained are presented in Table 4.

Table 4. Gibbs free energy and activation energy (kJ/mol) of the polymer chain growth stage for AS(I)-AS(IV).

Initial structure	ΔG^{\ddagger} (<i>trans-cis</i>)	ΔG (<i>trans-cis</i>)	ΔG^{\ddagger} (polymer)	ΔG^{\ddagger} (total)	ΔG (polymer)	Product
<i>i</i> -C ₄ H ₉ -CC-AS(I)-T	29.5	23.5	63.9	87.4	-15.0	<i>i</i> -C ₄ H ₉ -CCC-AS(I)
<i>i</i> -C ₄ H ₉ -CCC-AS(I)-T	28.9	23.3	64.0	87.3	-35.1	<i>i</i> -C ₄ H ₉ -CCCC-AS(I)
<i>i</i> -C ₄ H ₉ -CC-AS(I)-T			102.8	102.8	-58.7	<i>i</i> -C ₄ H ₉ -CCT-AS(I)
<i>i</i> -C ₄ H ₉ -CT-AS(I)-T	32.1	22.5	60.8	82.3	-18.4	<i>i</i> -C ₄ H ₉ -CTC-AS(I)

<i>i</i> -C ₄ H ₉ -CT-AS(I)-T			90.9	90.9	-56.6	<i>i</i> -C ₄ H ₉ -CTT-AS(I)
<i>i</i> -C ₄ H ₉ -CC-AS(II)-T	35.5	7.3	65.0	72.3	-21.3	<i>i</i> -C ₄ H ₉ -CCC-AS(II)
<i>i</i> -C ₄ H ₉ -CCC-AS(II)-T	34.0	7.6	63.7	71.3	-50.3	<i>i</i> -C ₄ H ₉ -CCCC-AS(II)
<i>i</i> -C ₄ H ₉ -CC-AS(II)-T			95.7	95.7	-53.7	<i>i</i> -C ₄ H ₉ -CCT-AS(II)
<i>i</i> -C ₄ H ₉ -CT-AS(II)-T	23.2	17.6	60.4	78.0	-29.0	<i>i</i> -C ₄ H ₉ -CTC-AS(II)
<i>i</i> -C ₄ H ₉ -CT-AS(II)-T			94.5	94.5	-2.2	<i>i</i> -C ₄ H ₉ -CTT-AS(II)
<i>i</i> -C ₄ H ₉ -CC-AS(III)-T	29.9	14.8	51.5	66.8	-27.3	<i>i</i> -C ₄ H ₉ -CCC-AS(III)
<i>i</i> -C ₄ H ₉ -CCC-AS(III)-T	29.5	7.6	51.8	59.4	-35.7	<i>i</i> -C ₄ H ₉ -CCCC-AS(III)
<i>i</i> -C ₄ H ₉ -CC-AS(III)-T			104.0	104.0	-51.7	<i>i</i> -C ₄ H ₉ -CCT-AS(III)
<i>i</i> -C ₄ H ₉ -CT-AS(III)-T	32.1	26.2	56.0	82.2	-2.8	<i>i</i> -C ₄ H ₉ -CTC-AS(III)
<i>i</i> -C ₄ H ₉ -CT-AS(III)-T			99.2	99.2	-25.3	<i>i</i> -C ₄ H ₉ -CTT-AS(III)
<i>i</i> -C ₄ H ₉ -CC-AS(IV)-T	24.6	14.6	51.7	66.3	-35.0	<i>i</i> -C ₄ H ₉ -CCC-AS(IV)
<i>i</i> -C ₄ H ₉ -CCC-AS(IV)-T	24.7	6.3	54.2	60.5	-60.4	<i>i</i> -C ₄ H ₉ -CCCC-AS(IV)
<i>i</i> -C ₄ H ₉ -CC-AS(IV)-T			102.0	102.0	-52.9	<i>i</i> -C ₄ H ₉ -CCT-AS(IV)
<i>i</i> -C ₄ H ₉ -CT-AS(IV)-T	21.4	12.9	70.1	83.0	-8.9	<i>i</i> -C ₄ H ₉ -CTC-AS(IV)
<i>i</i> -C ₄ H ₉ -CT-AS(IV)-T			77.5	77.5	-40.3	<i>i</i> -C ₄ H ₉ -CTT-AS(IV)

The analysis of the data presented in Table 4 can begin with a statement of the fact that for all model structures of active centers, the insertion of *trans*-1,3-butadiene into the reactive growing polymer chain occurs with a higher activation energy in comparison with the insertion of *cis*-1,3-butadiene, which occurs in two stages. When considering of the *cis*-1,4-polybutadiene reaction formation in the series AS(I), AS(II), AS(III), AS(IV), a consistent decrease in the total activation energy is observed. However, for AS(I) and AS(II) the total activation energy value is almost the same. In almost all cases, the growing polybutadiene chain with a terminal *trans*-unit turns out to be thermodynamically more stable than the growing polybutadiene chain with a terminal *cis*-unit. This indicates that when the rate of polymerization of 1,3-butadiene decreases, *anti-syn* isomerization of the terminal unit becomes possible. The results obtained are in good agreement with the experimental data of Table 1, namely an increase in the rate constant of the polymerization reaction and the content of *cis*-1,4-units in the polymer upon transition from AS(I) to AS(IV).

As noted above, all considered model active centers are *cis*-stereoregulatory. At the same time, the content of *trans*-1,4-units in polybutadiene can exceed 4.0% (Table 1). At the same time, for the physical and mechanical characteristics of the polymer, it is important how the "impurity" *trans*-1,4-units are distributed. A comparison of the total activation energies of reactions (3) and (4) shows that the bonding of the *cis*-1,3-butadiene to the terminal *cis*-unit of the growing polybutadiene chain occurs with a lower activation energy than the insertion to the terminal *trans*-unit for all types of active centers studied. For AS(IV), these activation energies are close, but the bonding of the *cis*-1,3-butadiene to the terminal *trans*-unit of the growing polybutadiene chain is somewhat more favorable. For the reaction (4) of the insertion of the *cis*-1,3-butadiene to the terminal *trans*-unit of the reactive growing polybutadiene chain, the total activation energy is almost the same for all active centers and is ~82 kJ/mol. This allows us to conclude that the appearance of a terminal *trans*-units in the growing polybutadiene chain in the case of AS(I), AS(II), and AS(III) should not lead to the appearance of the dyads of the *trans*-units. However, for AS(IV), the results obtained do not exclude the formation of small blocks of the *trans*-1,4 units.

It is also clear from the results in Table 4 that the total activation energies for the binding of 3 and 4 units to the polymer chain differ very slightly and are stabilized for each type of center at its own level. Thus, for AS(I), AS(II), AS(III), AS(IV) this is ~87, ~71, ~60 and ~61 kJ/mol, respectively.

Next, we will analyze the most characteristic, from our point of view, bond lengths between the Nd(III) ion and 1,3-butadiene, as well as between the Nd(III) ion and the terminal π -allylic units of the growing polymer chain for AS(I)-AS (IV) (Table 5). For convenience of presentation and discussion of materials, we will accept the following notations: C¹, C², C³ and C⁴ are the carbon atoms of coordinately bound 1,3-butadiene, and C ^{α} , C ^{β} , C ^{γ} and C ^{δ} are the carbon atoms of the terminal link of the growing polymer chain, where C¹ and C ^{α} are the carbon atoms closest to the lanthanide. The analysis of the geometry of the initial complexes *i*-C₄H₉-AS+ η -*trans*-C₄H₆, characteristic of the initiation stage, did not reveal fundamental differences in the molecular parameters for catalytic complexes with different chlorine contents. From Table 5, it follows that for all types of AS, the distance between Nd(III) and carbon atoms in the 1,3-butadiene in the *trans*-form is ~3 Å. This indicates that the main role in the binding of Nd(III) to the 1,3-butadiene is played by π -bonds, as well as electrostatic (dispersion and van der Waals) interactions.

Table 5. Characteristic distances between Nd(III), 1,3-butadiene and the growing polymer chain for the complexes *i*-C₄H₉-AS+ η -*trans*-C₄H₆ и *i*-C₄H₉-CCC-AS + η -*trans*-C₄H₆.

Characteristic distances, (R, Å)	AS (I)	AS (II)	AS (III)	AS (IV)
<i>i</i> -C ₄ H ₉ -AS+ η - <i>trans</i> -C ₄ H ₆ *				
R(Nd-C(<i>i</i> -C ₄ H ₉))	2.431	2.387	2.377	2.414
R(Nd-C ¹ (C ₄ H ₆))	3.504	3.244	3.261	3.513
R(Nd-C ² (C ₄ H ₆))	3.148	3.021	3.048	3.161
R(Nd-C ³ (C ₄ H ₆))	3.190	3.143	3.151	3.111
R(Nd-C ⁴ (C ₄ H ₆))	3.559	3.605	3.616	3.415
R(C ¹ (C ₄ H ₆)-C(<i>i</i> -C ₄ H ₉))	3.634	3.476	3.460	3.571
<i>i</i> -C ₄ H ₉ -CCC-AS + η - <i>trans</i> -C ₄ H ₆ **				
R(Nd-C ¹ (C ₄ H ₆))	3.295	3.380	3.309	3.161
R(Nd-C ² (C ₄ H ₆))	3.552	3.469	3.364	3.320
R(Nd-C ³ (C ₄ H ₆))	4.310	4.190	4.014	4.147
R(Nd-C ⁴ (C ₄ H ₆))	5.144	4.945	4.739	4.908
R(Nd-C ^{α} (C ₄ H ₆))	2.617	2.628	2.659	2.609
R(Nd-C ^{β} (C ₄ H ₆))	2.702	2.690	2.682	2.670
R(Nd-C ^{γ} (C ₄ H ₆))	2.732	2.751	2.672	2.758
R(Nd-C ^{δ} (C ₄ H ₆))	3.077	3.186	3.052	3.349
R(C ¹ (C ₄ H ₆)-C ^{α} (C ₄ H ₆))	3.302	3.324	3.427	3.359

* Full optimized structures (Cartesian coordinates of atoms) are in the supplementary materials, Table S1. ** Full optimized structures (Cartesian coordinates of atoms) are in the supplementary materials, Table S2.

For the chain growth stage, the geometry of the structures formed during the coordination of free 1,3-butadiene from the bulk of the reaction mixture to the *i*-C₄H₉-CCC-AS complex was calculated. Table 5 shows the structural characteristics for the complexes *i*-C₄H₉-CCC-AS(Mt)+ η -*trans*-C₄H₆. It should be noted that in this case the monomer is characterized by η -4-*trans* coordination in Nd(III), and the terminal link of the growing polymer chain is in the π -*anti*-configuration. The observed distances between Nd(III) and the carbon atoms of the monomer and the growing polymer chain for AS(I), AS(II), AS(III) and AS(IV) are close, i.e., do not depend on the chlorine content in AS.

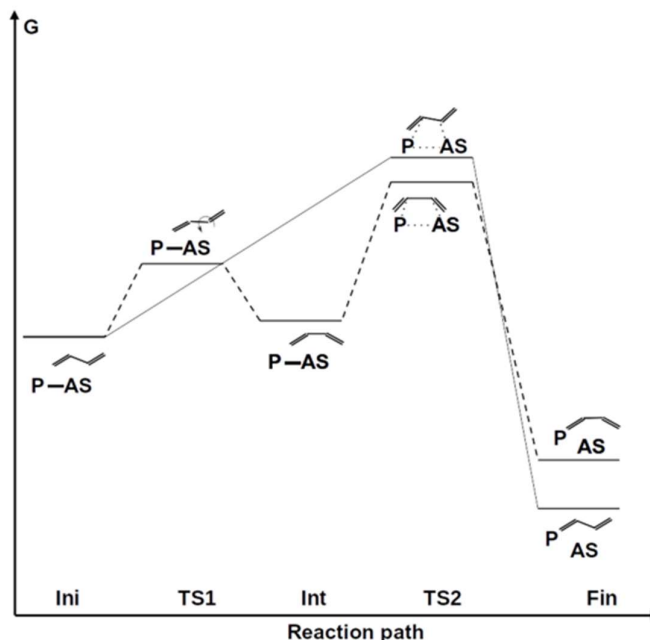


Figure 3. Energy diagram of the formation of 1,4-polybutadiene on AS, where P is $i\text{-C}_4\text{H}_9$ or the terminal π -allylic units of the growing polymer chain, **TS1** is the transition state due to the *trans-cis* transformation of 1,3-butadiene, **Int** is the intermediate of the *cis*-1,3-butadiene interacting with AS, **TS2** is a transition state caused by the incorporation 1,3-butadiene into the polymer chain.

4. Conclusions

Using previously obtained experimental data, theoretical modeling of the stereoregular polymerization of 1,3-butadiene catalyzed by the model active centers with different chlorine contents in the neodymium based Ziegler–Natta system was carried out. As a result, previously unknown peculiarities of the catalysis mechanism were obtained and substantiated. Thus, it was shown that structures with a high content of chlorine in a neodymium catalytic system should be more stable and active. The decrease in the concentration of active centers relative to the introduced Nd(III) at a [Cl]:[Nd] ratio of 3.0 or more is explained by the formation of structures inactive during the polymerization process, in which there is no possibility of the insertion of 1,3-butadiene into the reactive growing polymer chain.

For all considered model active centers during the 1,3-butadiene polymerization, the bonding of *trans*-1,3-butadiene to the reactive growing polymer chain occurs with a higher activation energy in comparison with the insertion of *cis*-1,3-butadiene. In this case, an increase in the [Cl]:[Nd] ratio is accompanied by a decrease in the activation barrier, which is consistent with an increase in the chain propagation rate constant and the content of *cis*-1,4 structures in the resulting polybutadiene. The higher thermodynamic stability of the terminal unit of the growing polymer chain in the *trans*-configuration confirms the possibility of the *anti-syn* isomerization process as a source of the formation of *trans*-1,4 structures in the polybutadiene during slow polymerization.

An important result is the analysis of the geometry of the complexes at the stages of initiation and growth of the polymer chain, where it was established that the reason for the difference in the activity of the complexes and their *cis*-stereospecificity is not the steric factor, but the energy route of the polymerization process.

Supplementary Materials: The following supporting information can be downloaded at the website of this paper posted on Preprints.org. Table S1: Atomic Cartesian coordinates (in Å) for optimized structures of $i\text{-C}_4\text{H}_9\text{-AS}+\eta\text{-trans-C}_4\text{H}_6$, Table S2: Atomic Cartesian coordinates (in Å) for optimized structures of $i\text{-C}_4\text{H}_9\text{-AS}+\eta\text{-trans-C}_4\text{H}_6$

Author Contributions: Conceptualization, Ildar G. Akhmetov and Ilsiya M. Davletbaeva; methodology, Alexey N. Masliy and Andrey M. Kuznetsov; software, Alexey N. Masliy; validation, Alexey N. Masliy, Ildar G. Akhmetov, Andrey M. Kuznetsov and Ilsiya M. Davletbaeva; formal analysis, Alexey N. Masliy and Ildar G. Akhmetov; investigation, Alexey N. Masliy and Ildar G. Akhmetov; resources, Andrey M. Kuznetsov; data curation, Alexey N. Masliy and Ildar G. Akhmetov; writing—original draft preparation, Alexey N. Masliy and Ildar G. Akhmetov; writing—review and editing, Andrey M. Kuznetsov and Ilsiya M. Davletbaeva; visualization, Alexey N. Masliy; supervision, Ilsiya M. Davletbaeva; project administration, Ildar G. Akhmetov and Ilsiya M. Davletbaeva.

Funding: This work was carried out within the framework of the current plan of scientific research of the University and is not supported by third-party funds.

Informed Consent Statement: Informed consent was obtained from all subjects involved in the study.

Institutional Review Board Statement: Not applicable.

Data Availability Statement: The data presented in this study are available on request from the corresponding author.

Conflicts of Interest: The authors declare no conflicts of interest.

References

1. Cooper, W., & Vaughan, G. (1967). Recent developments in the polymerization of conjugated dienes. *Progress in Polymer Science*, 1, 91-160. [https://doi.org/10.1016/0079-6700\(67\)90003-2](https://doi.org/10.1016/0079-6700(67)90003-2)
2. The stereo rubbers, William M. Saltman, Wiley-Interscience, New York, 1977, 897 pp. <https://doi.org/10.1002/pol.1978.130160112>
3. Hsieh, H. L., & Yeh, H. C. (1985). Polymerization of butadiene and isoprene with lanthanide catalysts; characterization and properties of homopolymers and copolymers. *Rubber Chemistry and Technology*, 58(1), 117-145. <https://doi.org/10.5254/1.3536054>
4. Marina, N. G., Monakov, Y. B., Sabirov, Z. M., & Tolstikov, G. A. (1991). Lanthanide compounds—Catalysts of stereospecific polymerization of diene monomers. Review. *Polymer science USSR*, 33(3), 387-417.
5. Friebe, L., Nuyken, O., & Obrecht, W. (2006). Neodymium-based Ziegler/Natta catalysts and their application in diene polymerization. *Neodymium Based Ziegler Catalysts—Fundamental Chemistry*, 1-154. https://doi.org/10.1007/12_094
6. Fischbach A, Anwander R. Neodymium Based Ziegler Catalysts Fundamental Chemistry. In: Nuyken O, ed. Berlin, Heidelberg: Springer, 2006. 204: 155–281. <https://doi.org/10.1007/11761013>
7. Zhang, Z., Cui, D., Wang, B., Liu, B., & Yang, Y. (2010). Polymerization of 1, 3-conjugated dienes with rare-earth metal precursors. *Molecular catalysis of rare-earth elements*, 49-108. https://doi.org/10.1007/430_2010_16
8. Wang, F., Liu, H., Hu, Y., & Zhang, X. (2018). Lanthanide complexes mediated coordinative chain transfer polymerization of conjugated dienes. *Science China Technological Sciences*, 61(9), 1286-1294. <https://doi.org/10.1007/s11431-018-9256-6>
9. Quirk, R. P., Kells, A. M., Yunlu, K., & Cuif, J. P. (2000). Butadiene polymerization using neodymium versatate-based catalysts: catalyst optimization and effects of water and excess versatic acid. *Polymer*, 41(15), 5903-5908. [https://doi.org/10.1016/S0032-3861\(99\)00775-2](https://doi.org/10.1016/S0032-3861(99)00775-2)
10. Kwag, G. (2002). A highly reactive and monomeric neodymium catalyst. *Macromolecules*, 35(13), 4875-4879. <https://doi.org/10.1021/ma012123p>
11. Zheng, W., Yang, Q., Dong, J., Wang, F., Luo, F., Liu, H., & Zhang, X. (2021). Neodymium-based one-precatalyst/dual-cocatalyst system for chain shuttling polymerization to access cis-1, 4/trans-1, 4 multiblock polybutadienes. *Materials Today Communications*, 27, 102453. <https://doi.org/10.1016/j.mtcomm.2021.102453>
12. Wang, H., Cue, J. M. O., Calubaquib, E. L., Kularatne, R. N., Taslimy, S., Miller, J. T., & Stefan, M. C. (2021). Neodymium catalysts for polymerization of dienes, vinyl monomers, and ϵ -caprolactone. *Polymer Chemistry*, 12(47), 6790-6823. <https://doi.org/10.1039/D1PY01270C>
13. Iovu, H., Hubca, G., Simionescu, E., Badea, E. G., & Dimonie, M. (1997). Polymerization of butadiene and isoprene with the NdCl₃-3TBP-TIBA catalyst system. *Die Angewandte Makromolekulare Chemie: Applied Macromolecular Chemistry and Physics*, 249(1), 59-77. <https://doi.org/10.1002/apmc.1997.052490105>
14. Srinivasa Rao, G. S., Upadhyay, V. K., & Jain, R. C. (1999). Polymerization of 1, 3-butadiene using neodymium chloride tripentanolate-triethyl aluminum catalyst systems. *Journal of applied polymer science*, 71(4), 595-602. [https://doi.org/10.1002/\(SICI\)1097-4628\(19990124\)71:4%3C595::AID-APP11%3E3.0.CO;2-7](https://doi.org/10.1002/(SICI)1097-4628(19990124)71:4%3C595::AID-APP11%3E3.0.CO;2-7)

15. Ren, C., Li, G., Dong, W., Jiang, L., Zhang, X., & Wang, F. (2007). Soluble neodymium chloride 2-ethylhexanol complex as a highly active catalyst for controlled isoprene polymerization. *Polymer*, 48(9), 2470-2474. <https://doi.org/10.1016/j.polymer.2007.02.027>
16. Hu, Y., Zhang, C., Liu, X., Gao, K., Cao, Y., Zhang, C., & Zhang, X. (2014). Methylaluminoxane-activated neodymium chloride tributylphosphate catalyst for isoprene polymerization. *Journal of Applied Polymer Science*, 131(8). <https://doi.org/10.1002/app.40153>
17. Kularatne, R. N., Yang, A., Nguyen, H. Q., McCandless, G. T., & Stefan, M. C. (2017). Neodymium catalyst for the polymerization of dienes and polar vinyl monomers. *Macromolecular Rapid Communications*, 38(19), 1700427. <https://doi.org/10.1002/marc.201700427>
18. Oehme, A., Gebauer, U., Gehrke, K., Beyer, P., Hartmann, B., & Lechner, M. D. (1994). The influence of the catalyst preparation on the homo-and copolymerization of butadiene and isoprene. *Macromolecular Chemistry and Physics*, 195(12), 3773-3781. <https://doi.org/10.1002/macp.1994.021951203>
19. Boisson, C., Barbotin, F., & Spitz, R. (1999). Polymerization of butadiene with a new catalyst based on a neodymium amide precursor. *Macromolecular Chemistry and Physics*, 200(5), 1163-1166. [https://doi.org/10.1002/\(SICI\)1521-3935\(19990501\)200:5%3C1163::AID-MACP1163%3E3.0.CO;2-O](https://doi.org/10.1002/(SICI)1521-3935(19990501)200:5%3C1163::AID-MACP1163%3E3.0.CO;2-O)
20. Friebe, L., Nuyken, O., Windisch, H., & Obrecht, W. (2002). Polymerization of 1, 3-Butadiene Initiated by Neodymium Versatate/Diisobutylaluminium Hydride/Ethylaluminium Sesquichloride: Kinetics and Conclusions About the Reaction Mechanism. *Macromolecular Chemistry and Physics*, 203(8), 1055-1064. [https://doi.org/10.1002/1521-3935\(20020501\)203:8%3C1055::AID-MACP1055%3E3.0.CO;2-H](https://doi.org/10.1002/1521-3935(20020501)203:8%3C1055::AID-MACP1055%3E3.0.CO;2-H)
21. Quirk, R. P., Kells, A. M. (2000). Polymerization of butadiene using neodymium versatate-based catalyst systems: preformed catalysts with SiCl₄ as halide source. *Polymer International*, 49(7), 751-756. [https://doi.org/10.1002/1097-0126\(200007\)49:7<751::AID-PI449>3.0.CO;2-K](https://doi.org/10.1002/1097-0126(200007)49:7<751::AID-PI449>3.0.CO;2-K)
22. Sigaeva, N. N., Usmanov, T. S., Budtov, V. P., & Monakov, Y. B. (2001). Effect of organoaluminum compound on kinetic nonuniformity and structure of active centers of neodymium catalytic systems in butadiene polymerization. *Russian journal of applied chemistry*, 74(7), 1141-1146. <https://doi:10.1023/A:1013019001878>
23. Monakov, Y. B., Sabirov, Z. M., Urazbaev, V. N., & Efimov, V. P. (2001). Relationship between the stereospecificity of lanthanide catalysts and the structures of active sites and dienes, the nature of a cocatalyst, and preparation conditions. *Kinetics and catalysis*, 42(3), 310-316. <https://doi:10.1023/A:1010453013151>
24. Sigaeva, N. N., Usmanov, T. S., Budtov, V. P., Spivak, S. I., Zaikov, G. E., & Monakov, Y. B. (2003). The influence of the nature of organoaluminum compound on kinetic heterogeneity of active sites in lanthanide-based diene polymerization. *Journal of applied polymer science*, 87(3), 358-368. <https://doi.org/10.1002/app.11172>
25. Monakov, Y. B., Sabirov, Z. M., Urazbaev, V. N., & Efimov, V. P. (2002). Diene polymerization initiated by NdCl₃. 3TBP-based catalytic systems. Multiplicity of active centers and their structure and stereospecificity distributions. *Polymer science. Series A*, 44(3), 228-231.
26. Urazbaev, V. N., Efimov, V. P., Sabirov, Z. M., & Monakov, Y. B. (2003). Structure of active centers, their stereospecificity distribution, and multiplicity in diene polymerization initiated by NdCl₃-based catalytic systems. *Journal of applied polymer science*, 89(3), 601-603. <https://doi.org/10.1002/app.11838>
27. Masliy, A. N., Akhmetov, I. G., Kuznetsov, A. M., & Davletbaeva, I. M. (2023). DFT and ONIOM Simulation of 1, 3-Butadiene Polymerization Catalyzed by Neodymium-Based Ziegler–Natta System. *Polymers*, 15(5), 1166. <https://doi.org/10.3390/polym15051166>
28. Masliy, A. N., Akhmetov, I. G., Kuznetsov, A. M., & Davletbaeva, I. M. (2024). Comparative ONIOM modeling of 1, 3-butadiene polymerization using Nd (III) and Gd (III) Ziegler–Natta catalyst systems. *International Journal of Quantum Chemistry*, 124(1), e27297. <https://doi.org/10.1002/qua.27297>
29. Akhmetov, I. G., Kozlov, V. G., Salakhov, I. I., Sakhabutdinov, A. G., & D'yakonov, G. S. (2010). Polymerisation kinetics and molecular characteristics of "neodymium" polybutadiene: influence of halogenating agent concentration. *International Polymer Science and Technology*, 37(3), 1-5. <https://doi.org/10.1177/0307174X10037003>
30. Salakhov, I. I., Akhmetov, I. G., & Kozlov, V. G. (2011). Polymerization of butadiene during the action of the catalytic system neodymium versatate-diisobutylaluminum hydride-hexachloro-p-xylene. *Polymer Science Series B*, 53(7), 385-390. <https://doi:10.1134/S1560090411070074>
31. Akhmetov, I. G. Sintez dienovyh kauchukov s ispol'zovaniem modificirovannyh kataliticheskikh sistem na osnove soedinenij neodima i litiya. Diss. dokt. chem. Nauk [Synthesis of diene rubbers using modified catalytic systems based on neodymium and lithium compounds. Dr. chem. sci. diss.]. Kazan, KNRTU Publ., 2013. 379 p.
32. Neese, F. (2012). The ORCA program system. *Wiley Interdisciplinary Reviews: Computational Molecular Science*, 2(1), 73-78. <https://doi.org/10.1002/wcms.81>
33. Neese, F. (2017). Software update: the ORCA program system, version 4.0. *Wiley Interdisciplinary Reviews-Computational Molecular Science*, 8(1), 73-78. <https://doi.org/10.1002/wcms.1327>

34. Dapprich, S., Komáromi, I., Byun, K. S., Morokuma, K., & Frisch, M. J. (1999). A new ONIOM implementation in Gaussian98. Part I. The calculation of energies, gradients, vibrational frequencies and electric field derivatives. *Journal of Molecular Structure: THEOCHEM*, 461, 1-21. [https://doi.org/10.1016/S0166-1280\(98\)00475-8](https://doi.org/10.1016/S0166-1280(98)00475-8)
35. Becke, A. Density-functional thermochemistry. III. The role of exact exchange (1993) *J. Chem. Phys.*, 98, 5648. <https://doi.org/10.1063/1.464913>
36. Lee, C., Yang, W., & Parr, R. G. (1988). Development of the Colle-Salvetti correlation-energy formula into a functional of the electron density. *Physical review B*, 37(2), 785. DOI: 10.1103/physrevb.37.785
37. Weigend, F., & Ahlrichs, R. (2005). Balanced basis sets of split valence, triple zeta valence and quadruple zeta valence quality for H to Rn: Design and assessment of accuracy. *Physical Chemistry Chemical Physics*, 7(18), 3297-3305. DOI: 10.1039/b508541a
38. Stoychev, G. L., Auer, A. A., & Neese, F. (2017). Automatic generation of auxiliary basis sets. *Journal of chemical theory and computation*, 13(2), 554-562. <https://doi.org/10.1021/acs.jctc.6b01041>
39. Dolg, M., Stoll, H., & Preuss, H. (1989). Energy-adjusted abinitio pseudopotentials for the rare earth elements. *The Journal of chemical physics*, 90(3), 1730-1734. <https://doi.org/10.1063/1.456066>
40. Grimme, S., Bannwarth, C., & Shushkov, P. (2017). A robust and accurate tight-binding quantum chemical method for structures, vibrational frequencies, and noncovalent interactions of large molecular systems parametrized for all spd-block elements (Z= 1–86). *Journal of chemical theory and computation*, 13(5), 1989-2009. <https://doi.org/10.1021/acs.jctc.7b00118>
41. Bannwarth, C., Ehlert, S., & Grimme, S. (2019). GFN2-xTB—An accurate and broadly parametrized self-consistent tight-binding quantum chemical method with multipole electrostatics and density-dependent dispersion contributions. *Journal of chemical theory and computation*, 15(3), 1652-1671. <https://doi.org/10.1021/acs.jctc.8b01176>
42. Grimme, S., Antony, J., Ehrlich, S., & Krieg, H. (2010). A consistent and accurate ab initio parametrization of density functional dispersion correction (DFT-D) for the 94 elements H-Pu. *The Journal of chemical physics*, 132(15), 154104. <https://doi.org/10.1063/1.3382344>
43. Ehlert, S., Stahn, M., Spicher, S., & Grimme, S. (2021). Robust and efficient implicit solvation model for fast semiempirical methods. *Journal of Chemical Theory and Computation*, 17(7), 4250-4261. <https://doi.org/10.1021/acs.jctc.1c00471>

Disclaimer/Publisher's Note: The statements, opinions and data contained in all publications are solely those of the individual author(s) and contributor(s) and not of MDPI and/or the editor(s). MDPI and/or the editor(s) disclaim responsibility for any injury to people or property resulting from any ideas, methods, instructions or products referred to in the content.